Heliyon 10 (2024) e27509

Contents lists available at ScienceDirect

Heliyon

journal homepage: www.cell.com/heliyon

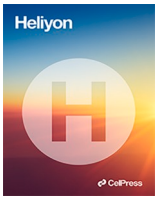

Research article

COVID-19 detection in lung CT slices using Brownian-butterfly-algorithm optimized lightweight deep features

Venkatesan Rajinikanth [a], Roshima Biju [b], Nitin Mittal [c,*], Vikas Mittal [d], S.S. Askar [e], Mohamed Abouhawwash [f]

[a] *Department of Computer Science and Engineering, Division of Research and Innovation, Saveetha School of Engineering, Saveetha Institute of Medical and Technical Sciences, Chennai, 602105, Tamil Nadu, India*
[b] *Department of Computer Science Engineering, Parul University, Vadodara, 391760, Gujarat, India*
[c] *Skill Faculty of Engineering and Technology, Shri Vishwakarma Skill University, Palwal, 121102, Haryana, India*
[d] *Department of Electronics and Communication Engineering, Chandigarh University, Mohali, 140413, India*
[e] *Department of Statistics and Operations Research, College of Science, King Saud University, P.O. Box 2455, Riyadh, 11451, Saudi Arabia*
[f] *Department of Mathematics, Faculty of Science, Mansoura University, Mansoura, 35516, Egypt*

ARTICLE INFO

Keywords:
COVID-19
Shannon's
MobileNet
Butterfly algorithm
Classification

ABSTRACT

Several deep-learning assisted disease assessment schemes (DAS) have been proposed to enhance accurate detection of COVID-19, a critical medical emergency, through the analysis of clinical data. Lung imaging, particularly from CT scans, plays a pivotal role in identifying and assessing the severity of COVID-19 infections. Existing automated methods leveraging deep learning contribute significantly to reducing the diagnostic burden associated with this process. This research aims in developing a simple DAS for COVID-19 detection using the pre-trained light-weight deep learning methods (LDMs) applied to lung CT slices. The use of LDMs contributes to a less complex yet highly accurate detection system. The key stages of the developed DAS include image collection and initial processing using Shannon's thresholding, deep-feature mining supported by LDMs, feature optimization utilizing the Brownian Butterfly Algorithm (BBA), and binary classification through three-fold cross-validation. The performance evaluation of the proposed scheme involves assessing individual, fused, and ensemble features. The investigation reveals that the developed DAS achieves a detection accuracy of 93.80% with individual features, 96% accuracy with fused features, and an impressive 99.10% accuracy with ensemble features. These outcomes affirm the effectiveness of the proposed scheme in significantly enhancing COVID-19 detection accuracy in the chosen lung CT database.

1. Introduction

Recent literature indicates a gradual increase in the incidence rate of the disease among the population, attributed to various factors. Infectious diseases pose a spectrum of challenges, ranging from mild to severe impacts on human health. Even with recommended precautionary measures in place, uncontrolled diseases have the potential to spread within large human groups. Therefore, timely and accurate detection, followed by appropriate treatment, is crucial to effectively address the condition and facilitate the

* Corresponding author.
E-mail addresses: v.rajinikanth@ieee.org (V. Rajinikanth), roshima2010@gmail.com (R. Biju), mittal.nitin84@gmail.com (N. Mittal), vikas.e14122@cumail.in (V. Mittal), saskar@ksu.edu.sa (S.S. Askar), abouhaww@msu.edu (M. Abouhawwash).

https://doi.org/10.1016/j.heliyon.2024.e27509
Received 18 May 2023; Received in revised form 29 February 2024; Accepted 29 February 2024
Available online 2 March 2024

patient's recovery through adherence to recommended medical protocols.

The SARS-CoV-2 virus, leading to COVID-19, has impacted individuals worldwide indiscriminately of their race, gender, or age, prompting the World Health Organization (WHO) to declare it a pandemic. The global scale of the crisis is reflected in the staggering numbers, with reported infections reaching 772,166,517 cases and a total death toll of 6,981,263, according to the most recent WHO report as of November 23, 2023 (source: https://covid19.who.int/) [1]. These figures underscore the significant mortality associated with COVID-19, emphasizing that despite the availability of vaccinations and medications, its prevalence remains challenging to control.

The literature evidents that the COVID-19 caused a large infection and death rate globally from year 2019 to till date. The earlier research related to the COVID-19 confirms that the Articifial Intelligence (AI) schemes played a vital role in screening, modelling and decision making process during the disease spread and still a number of AI schemes are used in clinics for COVID-19 infection examination tasks [2–5]. The common clinical practice involved in COVID-19 detection involves in; symptom examination, sample collection, Reverse Transcription-Polymerase Chain Reaction (RT-PCR) test for initial diagnosis and medical-imaging assisted confirmation of the infection and its severity [6–8]. The medical-imaging schemes, such as chest X-ray and CT slices are the common modalities considered to examine the lung infection due to COVID-19 and its analysis plays a prime role in confirming the severity of the lung infection, which plays a chief role in implementing the treatment to cure the disease with appropriate drugs.

Compared to the X-rays, the CT slices helps to get complete information regarding the lung infection. Further, the CT helps to provide a three-dimensional (3D) view of the lung and it helps to view the whole lung region using axial-, coronal- and sagittal-planes using a chosen 3D to 2D conversion. The earlier research on COVID-19 assessment confirm that the AI supported methods assisted the doctors during the lung evaluation in early 2020 when much information regarding the clinical protocol for COVID-19 was not developed. Hence, several AI-supported procedures like machine learning (ML) and deep learning (DL) methods are proposed to examine the CT slices. The COVID19 detection with pre-trained and customary DL methods employed a variety examination procedures to improve the detection accuracy dueing the lung CT examination [9–11].

Most of the earlier works in the literature considered the complex methods like high layered DL models, pre-processed CT slices, and integrated segmentation and classification methods to achieve a better accuracy on a chosen dataset [12,13]. Execution of these techniques needs a larger and complex computational power. Further, these methods needs larger training and validation time. Compared to the conventional DL methods, the lightweight deep learning methods (LDMs) are having a smaller structure, lesser initial paremeters to be tuned and provides a result which is close to the large structured DL methods. Due to this reasons, the LDMs are widely adopted by the researchers to detect the COVID-19 infection [11,12]. The integrated thresholding and DL supported classification discussed in Ref. [13] confirms that this scheme helps to achieve a better result compared to the raw image supported detection. Based on this motivation, proposed research also considered the Shannon's thresholding based image enhancement and LDM based classification of the chosen lung CT database.

The aim of this research is to develop a simple and more efficient disease assessment schemes (DAS) using the LDMs to detect the COVID1-19 infection from the thresholded lung CT slice database. The various phases of this DAS includes the following; (i) image resizing and enhancement using Shannon's entropy thresholding, (ii) deep features mining using a chosen LDM, (iii) features optimization using a novel Brownian Butterfly Algorithm (BBA), (iv) features fusion to generate a new features vector (DDF) and (v) binary classification and performance confirmation using three-fold cross-validation.

The main task of this work is to segregate the lung CT images into healthy/COVID-19 classes using the proposed DAS. For the experimental demonstration, this work considered 10000 2D axial-plane CT slices (5000 healthy and 5000 COVID19), and every image is then enhanced using Shannon's entropy based tri-level thresholding using the BBA. These images are then considered for the experimental investigation. The initial investigation is performed using the chosen LDMs with SoftMax classifier and based on the achieved performance, the necessary LDM is selected for the fused-features and ensemble-features generation. Along with the SoftMax, the detection performance is also verified using classifiers, like Random Forest (RF), Decision Tree (DT), Naïve Bayes (NB), K-Nearest Neighbour (KNN) and Support Vector Machine (SVM) are implemented, and classification performance is verified. This work employed the LDM architectures, like SqueezeNet (SN), SqueezeNext (SNe), NASNetMobile (NNM), MobileNetV1 (MN1), MobileNetV2 (MN2), MobileNetV3_Small (MN3S), and MobileNetV3_Large (MN3L) for the analysis, and the outcome of this scheme is tested using; individual, dual-deep features (DDF), and ensemble-deep features (EDF), and the results are compared. The research implemented with ensemble LDM features offered a classification accuracy of >99% with the Decision Tree (DT) classifier, which confirms the merit of the proposed technique.

The main contributions of this research include the following;

- Lung CT enhancement using Shannon's tri-level thresholding to improve the visibility of COVID-19 infection,
- Features extraction using LDM and optimization using Brownian Butterfly Algorithm (BBA)
- Execution of dual-deep feature-supported infection detection using dominant LDM features
- Implementation of ensemble deep features to improve COVID-19 detection accuracy.

The other regions of this paper are organized as follows; Section 2 presents the literature review, Section 3 demonstrates the methodology, and the results and conclusion are presented in Sections 4 and 5 correspondingly.

2. Literature review

Due to its implication, various DAS techniques are developed and implemented using ML and DL schemes to detectthe COVID-19

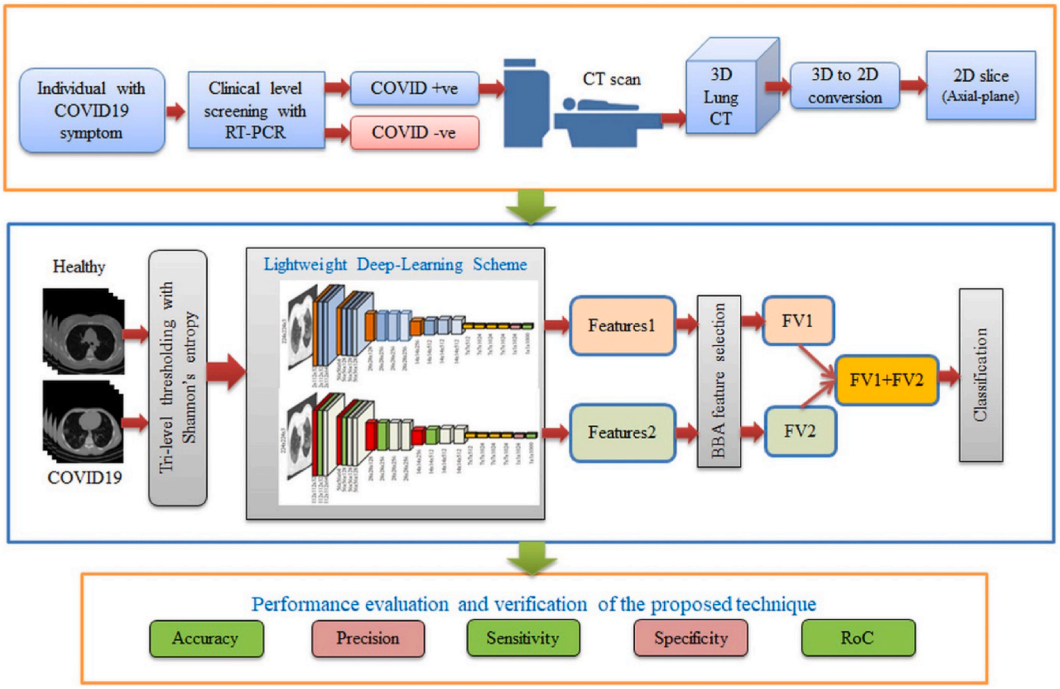

Fig. 1. Block diagram of the proposed approach.

infection using chosen imaging modality. Compared to the chest X-rays, the CT slice supported methods are very efficient in detecting the disease and its severity level to support the doctors in planning and implementing the necessary treatment to cure the disease.

COVID-19 detection with clinical and benchmark CT slices are widely discussed in the literature using pre-trained and customary DL methods. The previous works confirm that the DL-based examination provides better detection accuracy than conventional and ML schemes. Hence, several DL schemes are developed to support the COVID-19 segmentation/classification using lung CT slices of various planes. The summary of a few chosen existing procedures can be found in the review works and these methods confirms that the earlier methods provided a detection accuracy up to 100% [9–11].

The work of Furtado et al. (2022) implemented Cimatec-CovNet-19, a novel 3D supported LDM based on VGG16 scheme. This technique provided a detection accuracy of 90% when tested and verified on a balanced lung CT images with dimension 3000 [14]. Research by Bhosale and Patnaik (2022) discussed a low capacity hardware implementable LDM to classify the lung CT slices. This work is executed using Raspberry Pi integrated with a workstation and it achieved s detection accuracy of 99.28% [15]. Other related works existing in the literature for the examination of the lung CT slices helped to provide a detection accuracy up to 100% for the chosen image database [16,17].

The earlier works in the literature confism that the fused dual-deep fetaures (DDF) based approaches [18,19] and ensemble deep-features (EDF) approaches [20,21] helps to achieve a better COVID-19 detection compared to the individual features based techniques. To implement these techniques, it is necessary to identify the individual deep-features using an experimental study and the best feature vactors are then considered to implement the DDF and the EDF echnique.

Few earlier works in the literature confirms that the pre-processed CT images with a chosen thresholding approach helps to achieve a better detection accuracy compared to the raw images. Based on this motivation, this research work implemented a LDM based scheme on the raw and the thresholded images and the performance of the chosen procedures are initially verified using the individual features using the SoftMax. After identifying the best LDMs based on the result with the chosen CT database, the BBA based features optimization is implemented and the DDF is generated, Further, three LDMs based on its individual features performance is selected and EDF generation is implemented as discussed in Ref. [22]. Finally, the performance of the developed DAS is verified using individual, DDF and EDF using various binary classifiers and the achieved results are presented and discussed.

3. Materials and methods

The performance of the disease detection procedure depends mainly on the procedures employed in assessing the medical data. The complete information is presented in this section and this also presents the necessary information regarding methods employed to achieve the better detection accuracy.

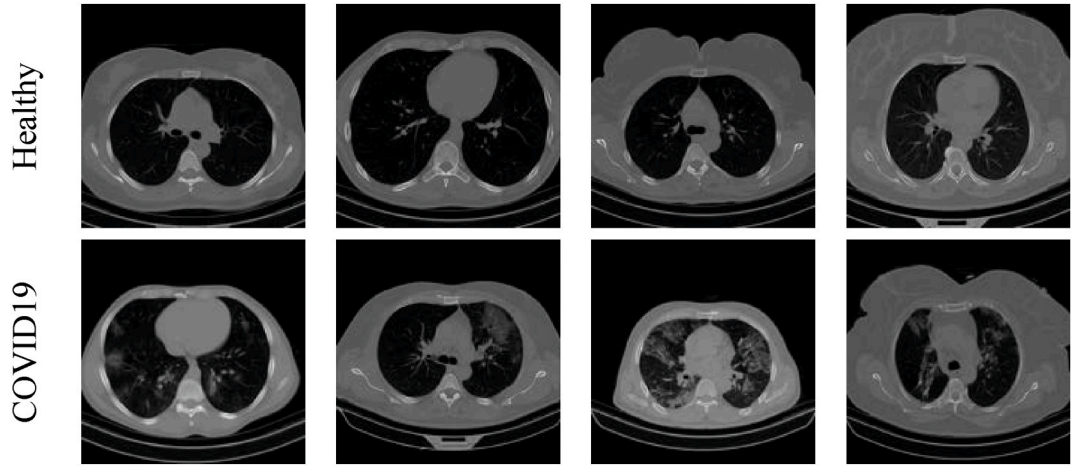

Fig. 2. Sample test images in chosen database.

3.1. Proposed scheme

This work considered the lung CT slices for the examination, and the procedure executed in this work is depicted in Fig. 1. A preliminary image collection is performed using the available database [23] containing 10000 images in axial-plane (5000 healthy images and 5000 COVID19 images) for assessment. In order to enhance the visibility of the lung region and its infection, each image is resized to $224 \times 224 \times 3$ pixels, noise removal is implemented to remove the unwanted pixels, and Shannon's Entropy tri-level thresholding is applied to pre-process the considered image slice. An enhanced image (Normal/COVID19) is then given to the LDM developed, which is trained using 80% of the data and validated and tested with 10% of the data.

To verify the performance of the chosen LDM, the classification task is initially performed using the SoftMax classifier with deep features. The proposed BBA is used to select features, and the DDF and EDF are employed to perform the classification task. Besides the SoftMax classifier, this study also considered binary classifiers such as RF, DT, NB, and SVM, and the results were evaluated. Three-fold cross-validation is employed in this study to verify the proposed scheme's performance, and its performance is compared with the existing literature results.

3.2. Image database

The test CT images for this research are collected from Ref. [23]. From its database, only 10000 CT slices (5000 healthy and 5000 COVID19) are considered for the investigation. Every image is considered for resizing, smoothening, and contrast improvement operations to get a preprocessed image to offer better detection accuracy with the chosen LDM. In this database, 80% of images are considered to train the developed scheme, 10% of data is for validation, and the remaining 10% is for the testing task. The results are then compared, and the proposed system's performance is verified. Fig. 2 depicts the sample pictures of this database.

The considered images are preprocessed using the Shannon's Entropy Thresholding (SET) with a chosen threshold value of three ($Th = 3$) to enhance the visibility of the lung and its infection.

3.2.1. Shannon's entropy thresholding

As the objective value of the SET, the goal is to maximize Shannon's entropy. The threshold selection by the BBA is performed until maximum entropy is obtained. The essential information regarding the SET is provided in Ref. [24].

Let us study a two-dimensional picture with size $x \times y$ in which $\int(x,y)$ indicates the pixels with distributions; $X\epsilon\{1,2,\ldots,x\}$ and $Y\epsilon\{1,2,\ldots,y\}$. If the image consist $L = 256$ thresholds, then the total thresholds in the image is $Th = \{1,2,\ldots,255\}$.

The image size and its threshold distribution can be represented as in Eqn. (1);

$$\int(x,y)\epsilon Th\forall(X,Y)\epsilon\ image \tag{1}$$

Let, $R = \{r_0, r_1, \ldots, r_{255}\}$ denotes the regulated image. Then the tri-level threshold selection ($Th = 3$) can be represented as in Eqn. (2);

$$R(Th) = \{r_0(th_1) + r_1(th_2) + r_2(th_3)\} \tag{2}$$

As an objective value, Shannon's entropy is maximized for each image and this value is obtained by using the proposed BBA. Its mathematical expression is given in Eqn. (3).

$$Th_{max} = \max\{R(Th) : for\ Th = 1\ to\ 255 \tag{3}$$

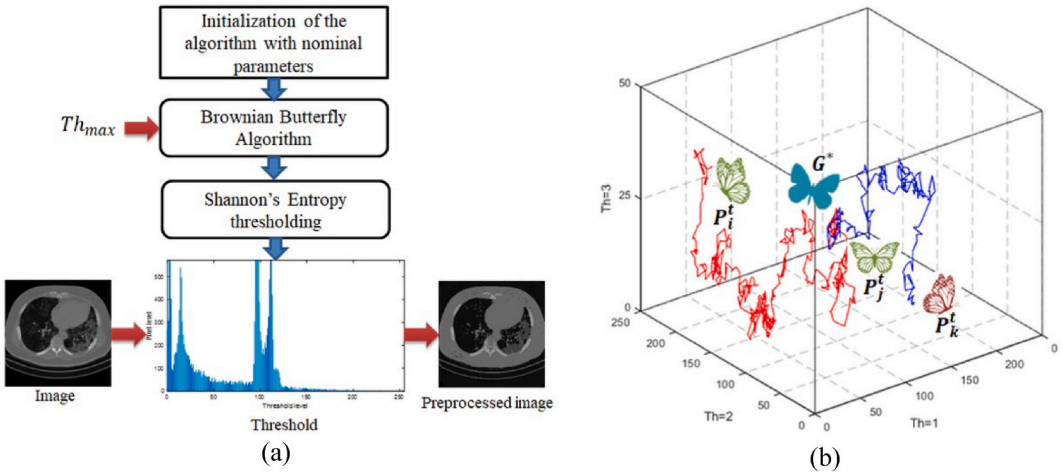

Fig. 3. Optimal thresholding (Th = 3) with Shannon's entropy and BBA (SE + BBA). (a) Implemented thresholding approach, and (b) BBA search in a 3D space.

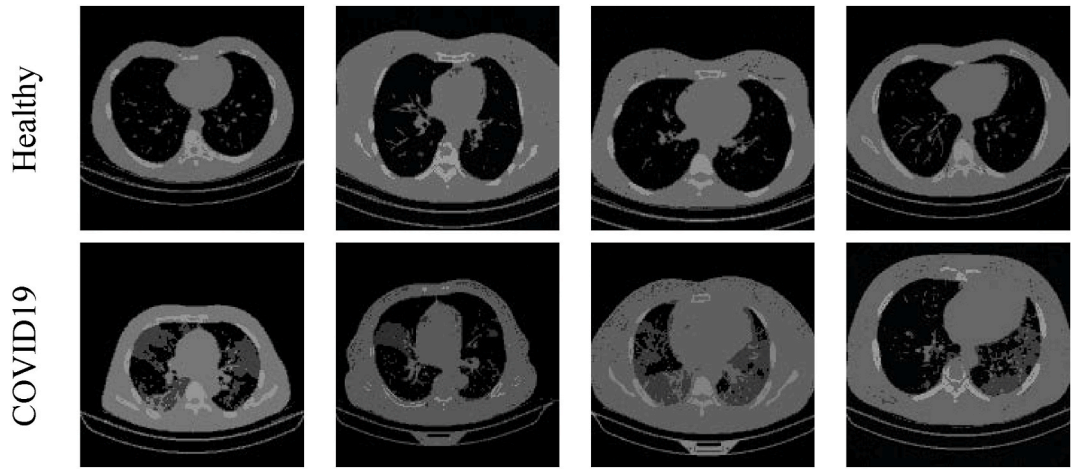

Fig. 4. Preprocessed lung CT slices with the chosen approach.

3.2.2. *Brownian Butterfly Algorithm*

Researchers have proposed a number of nature-inspired heuristic algorithms to find the best solution to a chosen tasks. For (i) Optimal threshold selection for preprocessing the test image and (ii) Optimal deep-feature collection using the LDM, the butterfly algorithm proposed by Arora and Singh (2019) is considered [25]. Unlike other approaches, this algorithm has simple initialization and updating functions that are easy to implement with fewer initial parameters, making it easier to implement. Further, to inspect the necessary solution from the CT slice, the Brownian-Walk (BW) search is executed. The BW operator improves the BA's performance by replacing the random search $\Re\epsilon\ [0,1]$ with a mathematically guided search. Further information regarding this scheme can be found at [26].

This algorithm is based on the movement of a butterfly towards dominated one, which releases a fragrance (F) as in Eqn. (4);

$$\mathsf{F} = cI^a \tag{4}$$

where I = intensity (0.8), c = modular modality (0.01) and a = power exponent with a value of $\epsilon\ [0.1, 0.3]$.

This algorithm integrates a straightforward global search space and a local search space to identify the optimal solution for the given problem. The position of a selected butterfly is represented by Eqns. (5) and (6). The global search, focused on exploration, aims to discover the dominant butterfly (G^*) within the designated search space, as outlined in Eqn. (5). Simultaneously, the local search, emphasizing exploitation, is illustrated by Eqn. (6). The effectiveness of both exploration and exploitation operations is monitored through a BW, aligning with the approach detailed in previous discussions, contributing to enhanced overall performance and results.

$$P_i^{t+1} = P_i^t + \left(\Re^2 \times G^* - P_i^t\right) \times BW \tag{5}$$

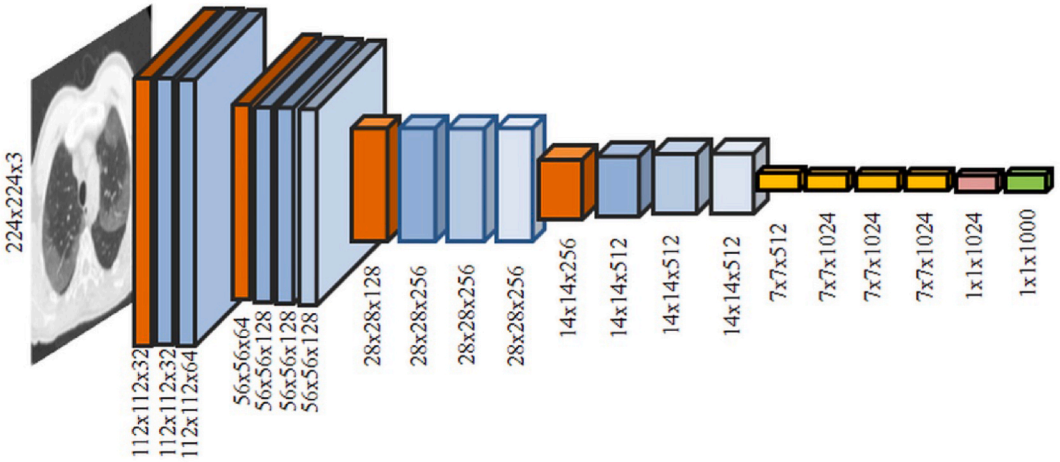

Fig. 5. Traditional MobileNetV1(MN1).

$$P_j^{t+1} = P_j^t + \left(\Re^2 \times P_k^t - P_j^t\right) \times BW \tag{6}$$

where P_i^t is primary spot of ith butterfly, P_i^{t+1} is the new spot of ith butterfly, P_j^t is primary spot of jth butterfly, P_k^t is primary spot of kth butterfly and P_j^{t+1} is the new spot of jth butterfly.

The BBA parameters are assigns as follows; total butterflies = 50, search dimension = 3 (ie. Th = 3), total iterations ($Iter_{max}$) = 2000 and search termination = Th_{max} or $Iter_{max}$). The implementation of the proposed work is shown in Fig. 3. Fig. 3(a) presents the implemented preprocessing work and Fig. 3(b) shows BBA search, which confirms that the proposed arrangement helps to achieve a better result on chosen CT slice. The sample enhanced results are depicted in Fig. 4 and these images are considered to verify the merit of proposed COVID-19 detection tool.

3.3. Lightweight deep-learning arrangement

According to recent research, several Machine Learning and Deep Learning algorithms have been implemented for detecting COVID19 infections with greater accuracy in lung CT/X-ray images. The earlier works further confirm that DL procedures outperform many cases due to its pixel-level exploration capabilities and the traditional pre-trained model alone sufficient to detect the disease in CT slices [27]. In order to verify the performance of the chosen DL model, high-end computational facilities are required for the implementation of conventional DL procedures. Based on the efforts of the researchers, LDM has been developed as a suitable alternative to conventional DL procedures in order to reduce this complexity. In LDM, computational effort is reduced, and most of these approaches can be implemented using mobile phones and low-capacity processing devices [28,29]. Fig. 5 illustrates the structure of MobiNetV1 and confirms that the proposed scheme is capable of delivering feature vector with size $1 \times 1 \times 1000$.

This research aims to implement the developed LDM scheme to examine the COVID19 infection in lung CT slices and verify the merit of the considered technique with a 3-fold cross-validation using; (i) individual, (ii) DDF, and (iii) EDF. It was observed that this study considered various LDM methods, such as SN, SNe, NNM, MN1, MN2, MN3S and ML3L [30–34]. provides information regarding these methods, and [35–39] provides preliminary software codes for this study.

This work considered the above-stated LDM for the examination, and every approach's performance is individually tested and verified based on the chosen data. Initially, individual features are used to verify performance. To obtain dual-deep features, two of the best LDMs are chosen, and serial feature integration is applied. As part of the ensemble feature procedure, the best feature from the chosen LDM is considered to determine a feature vector of dimension $1 \times 1 \times 1000$. The performance of the binary classification is then evaluated based on the metrics attained during the classification process.

3.4. Performance verification

To validate the importance of the DAS at the developmental level, it is necessary to confirm its performance with clinical-grade datasets. In this work, the merit of the developed LDM is verified using 1000 test images (500 healthy and 500 COVID19), and these images are considered as true-positive (TP) and true-negative (TN) information. When the implemented scheme detects a wrong value other than the TP and TN, it is then measured as false-positive (FP) and false-negative (FN), and these values will help to construct the confusion matrix based on other derived metrics, like accuracy (ACC), precision (PRE), sensitivity (SEN), and specificity (SPE). These values are considered to verify the merit of the executed tool, and the equations of these metrics measures are in Eqns. (7)–(10) [40–42]. These measures are separately computed for the classifiers, such as SoftMax, DT, RF, NB, and SVM. Along with these

measures, the Receiver Operating Characteristic (ROC) curve is also recorded.

The mathematical expression of these paremeters are presented in Eqns. (7)–(10);

$$ACC = \frac{TP + TN}{TP + TN + FP + FN} \times 100 \tag{7}$$

$$PRE = \frac{TP}{TP + FP} \times 100 \tag{8}$$

$$SEN = \frac{TP}{TP + FN} \times 100 \tag{9}$$

$$SPE = \frac{TN}{TN + FP} \times 100 \tag{10}$$

3.5. Implementation

The proposed scheme is implemented using a workstation having Intel i5, 12 GB Ram and 4 GB VRAM. The proposed experiment considered two softwares; PYTHON (3.11.1) and MATLAB (R2022b). MATLAB-software is considered to implement the BBA and Shannon's supported thresholding and the feature optimization process. The PYTHON-software is considered to implement the necessary deep-learning scheme and the classifier.

This section of the research presents the experimental results on each technique is presented and discussed individually. This work considered the pretrained schemes, such as SN, SNe, NNM, MN1, MN2, MN3S and MN3SL for the execution. The executed classification task considered 8000 images for training, 1000 images for validation and 1000 images for testing based on 3-fold cross-validation. The parameters of LDM schemes are assigned as follows; learning rate = 1×10^{-5}, Adam optimization, ReLu activation, total iteration = 1500, total epochs = 100, and SoftMax classifier as default unit.

This investigation is presented using individual, DDF and EDF with a dimension of $1 \times 1 \times 1000$ and the performance is verified based on the computed performance metrics. During the individual feature based classification, the outcome of the LDM depicted in Eqn. (11) is considered to verify the classification task. During the dual-deep feature, MN1 and MN3S are considered and the feature reduction is implemented using the BBA to find the best features by maximizing the Euclidean-Distance (ED) as shown in Eqn. (12). The LWD feature vector is shown in Eqn. (11) and the selected feature of this process is depicted in Eqns. (13) and (14) for two chosen LDM. The feature optimization procedure with heuristic algorithm is discussed in earlier works and in this research, the BBA is implemented to find optimal features and the selected features are serially concatenated to achieve the dual-deep features as in Eqn. (15), which is then considered to detect the COVID19 with netter accuracy compared to the individual features.

$$LDM_{(1\times1\times1000)} = LDM_{(1,1)}, LDM_{(1,2)}, \ldots, LDM_{(1,1000)} \tag{11}$$

$$ED(a,b)_{max} = \sqrt{\sum_{N=i}^{n} (a_N - b_N)^2} \tag{12}$$

where a and b are the two features in a search space (n) and a_N and b_N are the vectors.

$$MN1_{(1\times1\times351)} = MN1_{(1,1)}, MN1_{(1,2)}, \ldots, MN1_{(1,351)} \tag{13}$$

$$MN3S_{(1\times1\times407)} = MN3S_{(1,1)}, MN3S_{(1,2)}, \ldots, MN3S_{(1,407)} \tag{14}$$

$$DDF_{(1\times1\times758)} = MN1_{(1\times1\times351)} + MN3S_{(1\times1\times407)} \tag{15}$$

After finding the DDF using the proposed BBA, the necessary EDF are also computed in this work based on the recent work presented in Kundu et al. [22].

To select the ensemble features, the LDMs, such as MN1, MN2, and MN3S are considered. The best EDF vector is achieved using the necessary metrics, such as ACC, PRE, SEN, SPE, and AUC value and the selection of the EDF is and the necessary evaluation metrics (A^i) is developed by combining the chosen evaluation paremeters as in Eqn. (16);

$$A^i = \{ACC_i, PRE_i, SEN_i, SPE_i, AUC_i\} \tag{16}$$

Computation of the ensemble probability score is presented in Eqn. (17);

$$ens_j = \frac{\sum_i w^{(i)} \times p_j{}^{(i)}}{\sum_i w^{(i)}} \tag{17}$$

where ens_j = ensemble probability score, element weight $w^{(i)} = \sum_{x \epsilon A^i} \tanh(x)$, $rediction\ p_j{}^{(i)} = argmax(ens_j)$, $x \epsilon A^i$ = *element x chosen based on* A^i, and $\tanh(x)$ = *activation unit*.

Table 1
Classification results achieved for raw CT images using DMs and SoftMax.

LDM	TP	FN	TN	FP	ACC	PRE	SEN	SPE	ROC
SN	419	79	428	74	84.7000	84.9899	84.1365	85.2590	0.844
SNe	421	79	425	75	84.6000	84.8790	84.2000	85.0000	0.837
NNM	416	82	418	84	83.4000	83.2000	83.5341	83.2669	0.814
MN1	427	72	426	75	**85.3000**	**85.0598**	**85.5711**	**85.0299**	**0.849**
MN2	423	76	418	83	84.1000	83.5968	84.7695	83.4331	0.838
MN3S	424	76	426	74	85.0000	85.1406	84.8000	85.2000	0.845
MN3L	422	80	421	77	84.3000	84.5691	84.0637	84.5382	0.813

Table 2
Binary classification outcome with SoftMax classifier on thresholded CT images.

LDM	TP	FN	TN	FP	ACC	PRE	SEN	SPE	ROC
SN	453	39	447	61	90.0000	88.1323	92.0732	87.9921	0.906
SNe	461	41	455	43	91.6000	91.4683	91.8327	91.3655	0.912
NNM	459	40	456	45	91.5000	91.0714	91.9840	91.0180	0.911
MN1	445	35	489	31	**93.4000**	**93.4874**	**92.7083**	**94.0385**	**0.957**
MN2	457	40	468	35	92.5000	92.8862	91.9517	93.0417	0.913
MN3S	464	35	466	35	93.0000	92.9860	92.9860	93.0140	0.918
MN3L	461	40	463	36	92.4000	92.7565	92.0160	92.7856	0.912

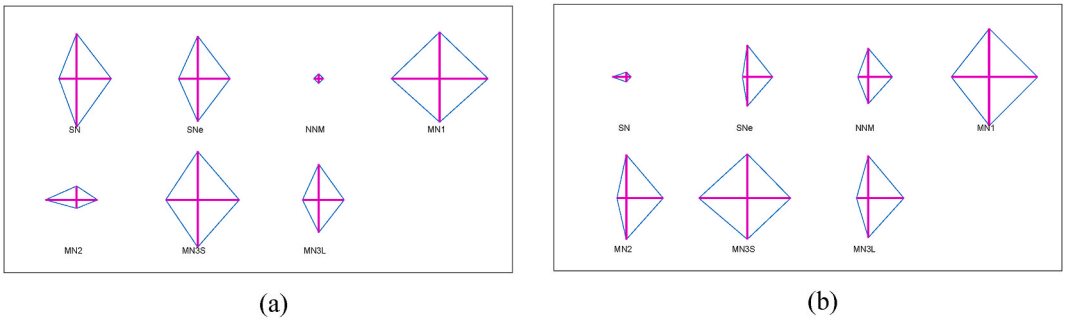

Fig. 6. Comparison of overall performance with Glyph-plot. (a) Raw CT slices, and (b) Pre-processed CT slices.

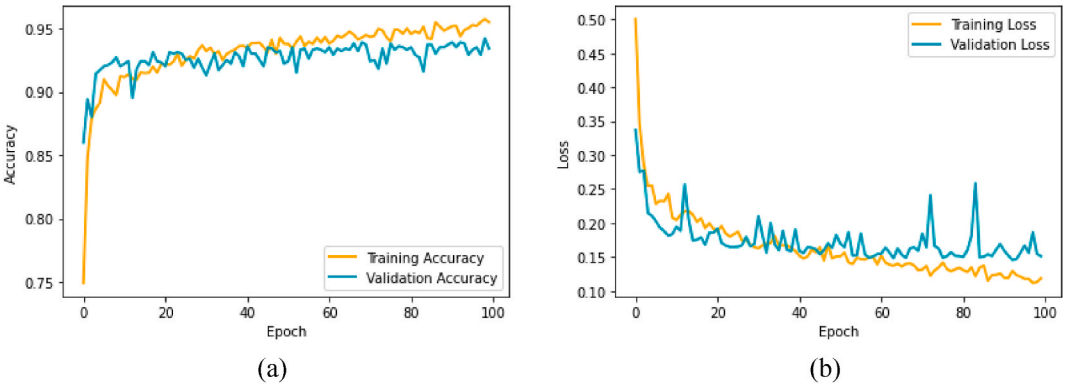

Fig. 7. Search convergence depicts the training and validation outcomes of MN1. (a) Accuracy, and (b) Loss.

4. Result and discussions

This section presents the experimental outcome achieved using Python software on a chosen workstation. Initially, the LDM with individual features is tested on the chosen lung CT database (10000 images), and the achieved results are presented and discussed. In this DAS, the binary classification task is executed using 3-fold cross-validation with SoftMax, and the best result achieved with each scheme is presented for discussion.

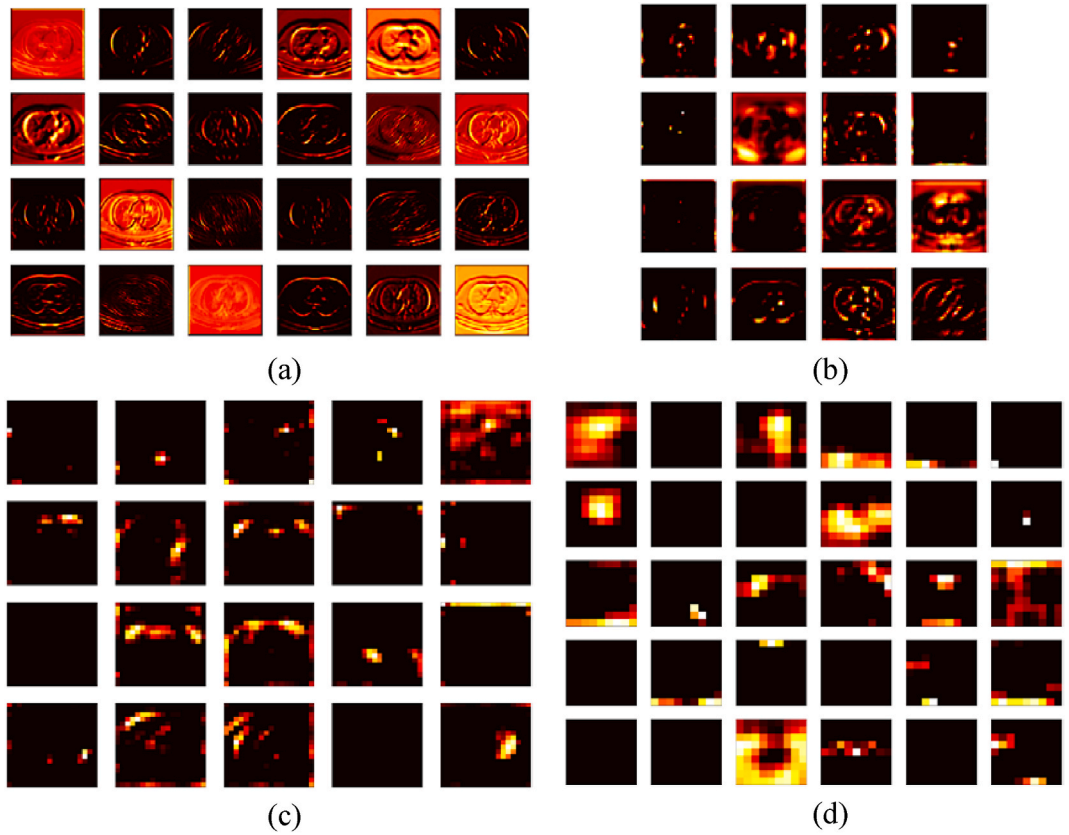

Fig. 8. Convolutional layer values for chosen image. (a) Convolution1, (b) Convolution2, (c) Convolution3, and (d) Convolution4.

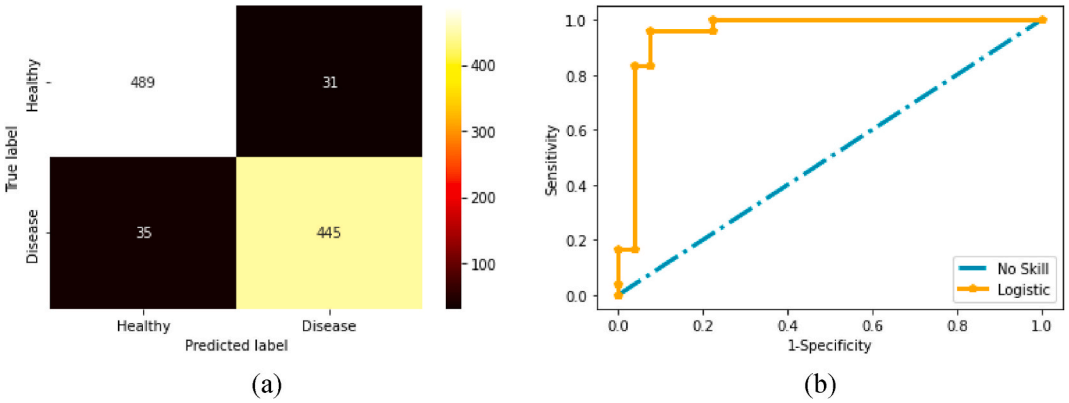

Fig. 9. Achieved results with MN1. (a) Confusion matrix, and (b) ROC curve.

Initially, the raw CT slices are considered for the investigation the achieved results during this task is depicted in Table 1. This table confiorms that the result by the MN1 is better compared to other schemes and it achieved an accuracy of 85.30%. Later, similar classification task is repeated using the pre-processed CT slices and the obtained results are shown in Table 2. This table confirms that the result of MN1 is better than other schemes, and MN3S presents a closer result than MN1. Further, Tables 1 and 2 results confirms that the COVID-19 detection performance is improved considerably when a pre-processed CT slices are considered. This confirms that the implemented SE + BBE based tri-level thresholding provides an enhanced result compared to the classification task implemented with the raw images. Fig. 6 presents the overall performance for Tables 1 and 2 values using the Glyph-plots, as in Fig. 6(a) and (b), respectively. These plots also verifies that the outcome of MN1 is superior compared to other LDMs of this study.

Fig. 7 presents the search convergence obtained with MN1 for the SoftMax classifier on the chosen database. Fig. 7(a) and (b) present the results for accuracy and loss, respectively, and this confirms that the training and validation values are close and confirm

Table 3
Overall result achieved with the proposed study.

Features	Classifier	TP	FN	TN	FP	ACC	PRE	SEN	SPE	ROC
MN1	SoftMax	459	37	472	32	93.1000	93.4827	92.5403	93.6508	0.921
	DT	472	38	450	40	92.2000	92.1875	92.5490	91.8367	0.933
	RF	468	37	455	40	92.3000	92.1260	92.6733	91.9192	0.942
	NB	466	38	458	38	92.4000	92.4603	92.4603	92.3387	0.947
	SVM	445	35	489	31	**93.4000**	**93.4874**	**92.7083**	**94.0385**	**0.957**
MN3S	SoftMax	464	35	466	35	93.0000	92.9860	92.9860	93.0140	0.918
	DT	468	35	463	34	93.1000	93.2271	93.0417	93.1590	0.937
	RF	470	32	466	32	93.6000	93.6255	93.6255	93.5743	0.952
	NB	469	30	467	34	93.6000	93.2406	93.9880	93.2136	0.928
	SVM	468	31	470	31	**93.8000**	**93.7876**	**93.7876**	**93.8124**	**0.9757**
DDF	SoftMax	479	23	472	26	95.1000	94.8515	95.4183	94.7791	0.961
	DT	479	22	475	24	95.4000	95.2286	95.6088	95.1904	0.969
	RF	477	20	477	26	95.4000	94.8310	95.9759	94.8310	0.972
	NB	476	24	480	20	95.6000	95.9677	95.2000	96.0000	0.970
	SVM	481	20	479	20	**96.0000**	**96.0080**	**96.0080**	**95.9920**	**0.979**
EDF	SoftMax	487	14	487	12	97.4000	97.5952	97.2056	97.5952	0.987
	DT	488	118	490	11	97.8000	97.7956	97.7956	97.8044	0.985
	RF	495	6	496	3	**99.1000**	**99.3976**	**98.8024**	**99.3988**	**0.993**
	NB	493	7	491	9	98.4000	98.2072	98.6000	98.2000	0.989
	SVM	492	9	491	8	98.3000	98.4000	98.2036	98.3968	0.990

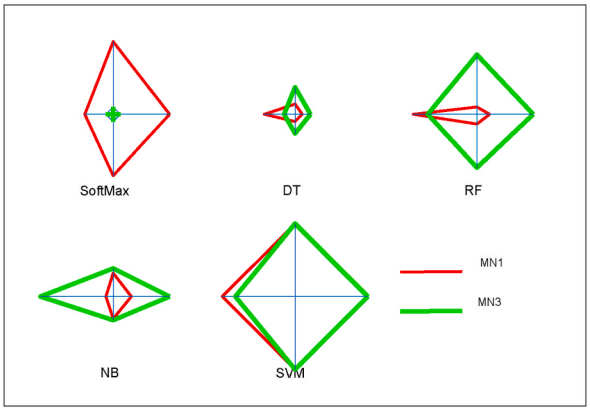

Fig. 10. The combined Glyph-Plot for MN1 and MN3S is considered to verify the best classifier.

the merit of the proposed scheme. The intermediate layer results for MN1 are depicted in Fig. 8. Fig. 8(a)–8(d) represent the outcome for a chosen image with convolutional layers 1 to 4, confirming that the considered picture is transferred into features with these operations. After the fully connected layers, it helps to get a feature vector of dimension. Fig. 9 depicts the outcome in which Fig. 9(a) shows the confusion matrix, and Fig. 9(b) presents the ROC curve. Similar outcomes are achieved in all other methods considered in the research work.

After verifying the individual performance of the chosen LDM, the merit of the MN1 and MN3 is confirmed with other chosen classifiers, like DT, RF, NB, and SVM. The achieved results are registered in Table 3. Then, the integrated features of MN1 and MN3S are considered to form the dual-deep features, and their performance is also verified with the chosen classifiers. Finally, the performance of the proposed approach is tested using the ensemble features, and the outcome achieved with this task helped achieve a better classification accuracy than other schemes considered in this work. This confirms that the ensemble features-supported approach provides a better result with RF (>99%), and this result is then verified with the other similar outcomes adopted from the literature.

To verify the performance of the proposed scheme, a graphical comparison of Table 3 is presented and initially the performance of MN1 and MN3S is verified using the combined Glyph-Plot as depicted in Fig. 10. The larger pattern is the best value and this confirms that the SVM classifier offers a better overall performance compared to the other classifiers considered in this study. To verify the results by DDF and the EDF, spider-plot based comparison is presented as in Fig. 11. Fig. 11(a) presents the outcome of the DDF and this confirms that the SVM classifier offers a better result and Fig. 11(b) presents the performance with EDF and it confirms that the RF classifier provides a better result. This study verifies that the EDF based COVID-19 offers a better outcome compared to other features considered in this study.

This work implements an LDM scheme to classify the lung CT slices into healthy/COVID-19 class, and the achieved results are verified. The significant merit of this scheme is, it implements the pre-trained LDMs to achieve a detection accuracy of >93% with the chosen technique and helps to achieve an accuracy up to 99.10% with the EDF. In this work, the SE + BBA based thresholding is

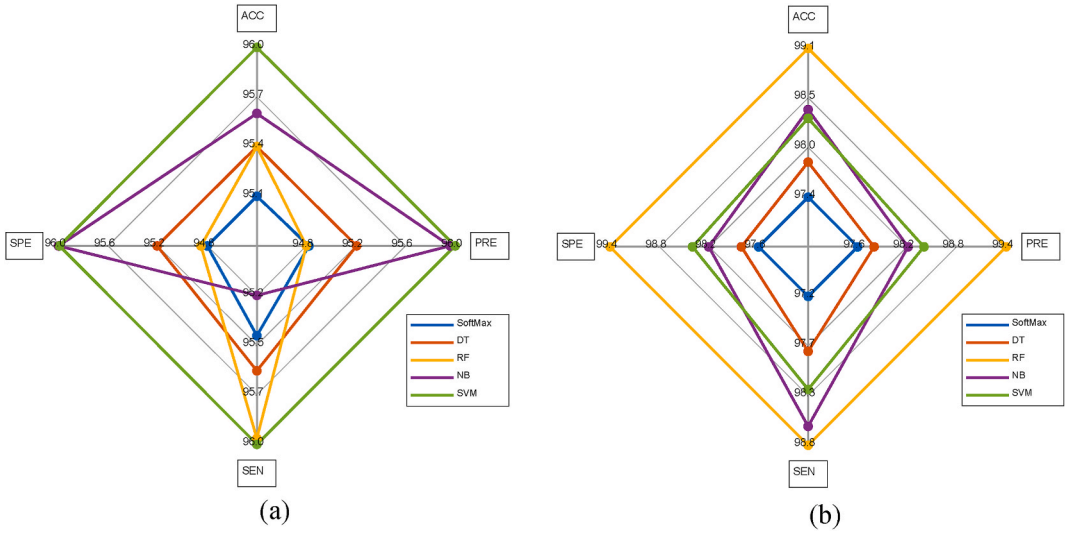

Fig. 11. Spider-plot to verify the performance of DDF and EDF based classification. (a) DDF, and (b) EDF.

implemented to enhance the test image and in future, the performance of this technique can be verified with othetr thresholding and heuristic algorithms found in the literature. The developed scheme is simple and it needs a LDM to obtain a satisfactory COVOD-19 detection accuracy. In future, its merit and clinical significance can be verified bt considering the clinically collected CT slices.

5. Conclusion

As a medical emergency, COVID19 requires prompt consideration and treatment. Using a binary classifier with cross-validation three times, this study proposed an LDM scheme for classifying lung CT slices into healthy/COVID-19 classes. 2D lung CT slices (10,000 numbers) are considered for the examination in the proposed work to improve detection accuracy. This work initially implements SE + BBA based thresholding task to enhance the visibil; ityof the chosen CT slices and the pre-processed images are then considered to verify the performance of the developed DAS. The experimental investigation is implemented by considering the raw and thresholded CT slices and this result confirms a considerable improvement in detection accuracy when the preprocessed CT images are considered. Initially, individual features based classification is implemented to identify the best LDMs (MN1 and MN3S) and these features are then optimized with BBA and the DDF are generated using the serial features fusion. Along with the DDF, this work also generated the EDF using the best features of MN1, MN2 and MN3S. The image classification task is separately executed using individual, DDF, and EDF using different binary classifiers and the outcome of this investigation confirmed that the EDF with RF classifier provided a better accuracy (99.10%) when thresholded CT images are considered. The over result of this study confirms that the proposed pre-trained LDM based DAS woks well on the chosen image database. In future, its merit can be verified using the clinically collected CT slices.

Ethical approval

This article does not contain any studies with human participants or animals performed by any of the authors.

Informed consent

Informed consent was obtained from all individual participants included in the study.

Data availability statements

The lung CT image database considered in this research work can be accessed from "https://www.kaggle.com/code/hosseinsholehrasa/covid-non-covid-custom-cnn-network/data".

Funding

This project is funded by King Saud University, Riyadh, Saudi Arabia.

CRediT authorship contribution statement

Venkatesan Rajinikanth: Writing – original draft, Software, Methodology, Investigation, Conceptualization. **Roshima Biju:** Writing – original draft, Software, Resources. **Nitin Mittal:** Writing – review & editing, Validation. **Vikas Mittal:** Writing – review & editing. **S.S. Askar:** Writing – review & editing, Visualization, Project administration. **Mohamed Abouhawwash:** Writing – review & editing.

Declaration of competing interest

The authors declare that they have no known competing financial interests or personal relationships that could have appeared to influence the work reported in this paper.

Acknowledgements

Researchers Supporting Project number (RSP2024R167), King Saud University, Riyadh, Saudi Arabia.

References

[1] https://covid19.who.int/.
[2] L. Song, X. Liu, S. Chen, S. Liu, X. Liu, K. Muhammad, S. Bhattacharyya, A deep fuzzy model for diagnosis of COVID-19 from CT images, Appl. Soft Comput. 122 (2022) 108883.
[3] C. Wen, S. Liu, S. Liu, A.A. Heidari, M. Hijji, C. Zarco, K. Muhammad, ACSN: attention capsule sampling network for diagnosing COVID-19 based on chest CT scans, Comput. Biol. Med. 153 (2023) 106338.
[4] X. Liu, Y. Liu, W. Fu, S. Liu, SCTV-UNet: a COVID-19 CT segmentation network based on attention mechanism, Soft Comput. (2023) 1–11.
[5] R. Pu, S. Liu, X. Ren, D. Shi, Y. Ba, Y. Huo, N. Cheng, The screening value of RT-LAMP and RT-PCR in the diagnosis of COVID-19: systematic review and meta-analysis, J. Virol Methods 300 (2022) 114392.
[6] P. Afshar, S. Heidarian, N. Enshaei, F. Naderkhani, M.J. Rafiee, A. Oikonomou, A. Mohammadi, COVID-CT-MD, COVID-19 computed tomography scan dataset applicable in machine learning and deep learning, Sci. Data 8 (1) (2021) 1–8.
[7] Y. Song, S. Zheng, L. Li, X. Zhang, X. Zhang, Z. Huang, Y. Yang, Deep learning enables accurate diagnosis of novel coronavirus (COVID-19) with CT images, IEEE ACM Trans. Comput. Biol. Bioinf 18 (6) (2021) 2775–2780.
[8] A. Narin, C. Kaya, Z. Pamuk, Automatic detection of coronavirus disease (covid-19) using x-ray images and deep convolutional neural networks, Pattern Anal. Appl. 24 (3) (2021) 1207–1220.
[9] Z.A.A. Alyasseri, M.A. Al-Betar, I.A. Doush, M.A. Awadallah, A.K. Abasi, S.N. Makhadmeh, R.A. Zitar, Review on COVID-19 diagnosis models based on machine learning and deep learning approaches, Expet Syst. 39 (3) (2022) e12759.
[10] T.A. Soomro, L. Zheng, A.J. Afifi, A. Ali, M. Yin, J. Gao, Artificial intelligence (AI) for medical imaging to combat coronavirus disease (COVID-19): a detailed review with direction for future research, Artif. Intell. Rev. 55 (2) (2022) 1409–1439.
[11] A.M. Mosa, E.A. Hamed, Z. Hussein, R.A. Jaleel, Improved smart forecasting model to combat coronavirus using machine learning, in: 2022 2nd International Conference on Advance Computing and Innovative Technologies in Engineering (ICACITE), IEEE, 2022, April, pp. 1953–1957.
[12] A.S. Al-Waisy, S. Al-Fahdawi, M.A. Mohammed, K.H. Abdulkareem, S.A. Mostafa, M.S. Maashi, B. Garcia-Zapirain, COVID-CheXNet: hybrid deep learning framework for identifying COVID-19 virus in chest X-rays images, Soft Comput. (2020) 1–16.
[13] S. Goyal, R. Singh, Detection and classification of lung diseases for pneumonia and Covid-19 using machine and deep learning techniques, J. Ambient Intell. Hum. Comput. (2021) 1–21.
[14] A. Furtado, C.A.C. da Purificação, R. Badaró, E.G.S. Nascimento, A light deep learning algorithm for CT diagnosis of COVID-19 pneumonia, Diagnostics 12 (7) (2022) 1527.
[15] Y.H. Bhosale, K.S. Patnaik, IoT deployable lightweight deep learning application for COVID-19 detection with lung diseases using RaspberryPi, in: 2022 International Conference on IoT and Blockchain Technology (ICIBT), IEEE, 2022, May, pp. 1–6.
[16] A. Abuhamdah, G.M. Jaradat, M. Alsmadi, Deep learning for COVID-19 cases-based XCR and chest CT images, in: Advances on Smart and Soft Computing, Springer, Singapore, 2022, pp. 285–299.
[17] Y. Kaya, E. Gürsoy, A MobileNet-based CNN model with a novel fine-tuning mechanism for COVID-19 infection detection, Soft Comput. (2023) 1–15.
[18] S.R. Nayak, D.R. Nayak, U. Sinha, V. Arora, R.B. Pachori, Application of deep learning techniques for detection of COVID-19 cases using chest X-ray images: a comprehensive study, Biomed. Signal Process Control 64 (2021) 102365.
[19] H. Mukherjee, S. Ghosh, A. Dhar, S.M. Obaidullah, K.C. Santosh, K. Roy, Deep neural network to detect COVID-19: one architecture for both CT Scans and Chest X-rays, Appl. Intell. 51 (5) (2021) 2777–2789.
[20] S. Tiwari, A. Jain, A lightweight capsule network architecture for detection of COVID-19 from lung CT scans, Int. J. Imag. Syst. Technol. 32 (2) (2022) 419–434.
[21] A.A. Ardakani, A.R. Kanafi, U.R. Acharya, N. Khadem, A. Mohammadi, Application of deep learning technique to manage COVID-19 in routine clinical practice using CT images: results of 10 convolutional neural networks, Comput. Biol. Med. 121 (2020) 103795.
[22] R. Kundu, R. Das, Z.W. Geem, G.T. Han, R. Sarkar, Pneumonia detection in chest X-ray images using an ensemble of deep learning models, PLoS One 16 (9) (2021) e0256630.
[23] https://www.kaggle.com/code/hosseinsholehrasa/covid-non-covid-custom-cnn-network.
[24] V. Rajinikanth, K. Palani Thanaraj, S.C. Satapathy, S.L. Fernandes, N. Dey, Shannon's entropy and watershed algorithm based technique to inspect ischemic stroke wound, in: Smart Intelligent Computing and Applications, Springer, Singapore, 2019, pp. 23–31.
[25] S. Arora, S. Singh, Butterfly optimization algorithm: a novel approach for global optimization, Soft Comput. 23 (3) (2019) 715–734.
[26] N. Sri Madhava Raja, V. Rajinikanth, K. Latha, Otsu based optimal multilevel image thresholding using firefly algorithm, Model, Simulat. Eng. 2014 (2014) 1–17.
[27] T. Zhou, H. Lu, Z. Yang, S. Qiu, B. Huo, Y. Dong, The ensemble deep learning model for novel COVID-19 on CT images, Appl. Soft Comput. 98 (2021) 106885.
[28] T. Sanida, A. Sideris, D. Tsiktsiris, M. Dasygenis, Lightweight neural network for COVID-19 detection from chest X-ray images implemented on an embedded system, Technologies 10 (2) (2022) 37.
[29] A. Verma, S.B. Amin, M. Naeem, M. Saha, Detecting COVID-19 from chest computed tomography scans using AI-driven android application, Comput. Biol. Med. 143 (2022) 105298.
[30] F.N. Iandola, S. Han, M.W. Moskewicz, K. Ashraf, W.J. Dally, K. Keutzer, SqueezeNet: AlexNet-Level Accuracy with 50x Fewer Parameters And< 0.5 MB Model Size, 2016 *arXiv preprint arXiv:1602.07360*.
[31] A. Gholami, K. Kwon, B. Wu, Z. Tai, X. Yue, P. Jin, K. Keutzer, Squeezenext: hardware-aware neural network design, in: Proceedings of the IEEE Conference on Computer Vision and Pattern Recognition Workshops, 2018, pp. 1638–1647.

[32] A.G. Howard, M. Zhu, B. Chen, D. Kalenichenko, W. Wang, T. Weyand, H. Adam, Mobilenets: Efficient Convolutional Neural Networks for Mobile Vision Applications, 2017 *arXiv preprint arXiv:1704.04861*.
[33] M. Sandler, A. Howard, M. Zhu, A. Zhmoginov, L.C. Chen, Mobilenetv2: inverted residuals and linear bottlenecks, in: Proceedings of the IEEE Conference on Computer Vision and Pattern Recognition, 2018, pp. 4510–4520.
[34] A. Howard, M. Sandler, G. Chu, L.C. Chen, B. Chen, M. Tan, H. Adam, Searching for mobilenetv3, in: Proceedings of the IEEE/CVF International Conference on Computer Vision, 2019, pp. 1314–1324.
[35] https://github.com/cmasch/squeezenet.
[36] https://github.com/rcmalli/keras-squeezenet.
[37] https://github.com/Sakib1263/MobileNet-1D-2D-Tensorflow-Keras.
[38] https://github.com/xiaochus/MobileNetV2.
[39] https://github.com/xiaochus/MobileNetV3.
[40] M. Heidari, S. Mirniaharikandehei, A.Z. Khuzani, G. Danala, Y. Qiu, B. Zheng, Improving the performance of CNN to predict the likelihood of COVID-19 using chest X-ray images with preprocessing algorithms, Int. J. Med. Inf. 144 (2020) 104284.
[41] M. Polsinelli, L. Cinque, G. Placidi, A light CNN for detecting COVID-19 from CT scans of the chest, Pattern Recogn. Lett. 140 (2020) 95–100.
[42] N. Subramanian, O. Elharrouss, S. Al-Maadeed, M. Chowdhury, A review of deep learning-based detection methods for COVID-19, Comput. Biol. Med. (2022) 105233.